



Orthogonal Genetic Algorithm Based Power System Restoration Path Optimization

Xie, Yunyun; Kunlong, Song ; Wu, Qiuwei

Published in:
International Transactions on Electrical Energy Systems

Link to article, DOI:
[10.1002/etep.2630](https://doi.org/10.1002/etep.2630)

Publication date:
2018

Document Version
Peer reviewed version

[Link back to DTU Orbit](#)

Citation (APA):
Xie, Y., Kunlong, S., & Wu, Q. (2018). Orthogonal Genetic Algorithm Based Power System Restoration Path Optimization. *International Transactions on Electrical Energy Systems*, 28(12), [e2630].
<https://doi.org/10.1002/etep.2630>

General rights

Copyright and moral rights for the publications made accessible in the public portal are retained by the authors and/or other copyright owners and it is a condition of accessing publications that users recognise and abide by the legal requirements associated with these rights.

- Users may download and print one copy of any publication from the public portal for the purpose of private study or research.
- You may not further distribute the material or use it for any profit-making activity or commercial gain
- You may freely distribute the URL identifying the publication in the public portal

If you believe that this document breaches copyright please contact us providing details, and we will remove access to the work immediately and investigate your claim.

Orthogonal Genetic Algorithm Based Power System Restoration Path Optimization

Xie Yunyun^{1*}, Song Kunlong^{2,1}, Wu Qiuwei³

1 Nanjing University of Science and Technology, Nanjing 210094, Jiangsu Province, China

2 Guodian Science and Technology Research Institute, Chengdu 610041, Sichuan Province, China

3 Centre for Electric Power and Energy System, Department of Electrical Engineering, Technical University of Denmark, Kgs. Lyngby, 2800, Denmark

Abstract: Optimizing the power system restoration path is a key issue for the system restoration after a blackout. Because the optimization is a complex nonlinear programming problem, artificial intelligent algorithms are widely employed to solve this problem due to its modeling flexibility and strong optimization capability. However, because the dimension of restoration path optimization is very high especially for large scale systems, artificial intelligent algorithms in current works are easy to be trapped in the local optima. In order to improve the optimal solution from the artificial intelligence algorithms, an orthogonal genetic algorithm is employed in this paper to optimize the restoration path, which can search the solution space in a statistically sound manner. Firstly, the experimental design method was employed to generate orthogonal array as the initial population which was scattered uniformly over the feasible solution space. Then, the orthogonal crossover operator based on the orthogonal experimental design was employed to generate a small but representative feasible solution as the potential offspring. Finally, the proposed method is validated using the IEEE 118-bus test system and part of the Jiangsu power grid in China.

Keywords: Orthogonal experimental design, orthogonal genetic algorithm, path optimization, power system restoration.

1. Introduction

With rapid development of modern society and economy, reliable and secure power supply has to be ensured. Although the robustness of large-scale power grids against cascading failures has been enhanced by advanced operation and control technologies developed in last decades [1], there still exists the possibility of large scale blackouts, such as the Northeastern Blackout of United States and Canada in 2003 [2] and the India blackout in 2012 [3]. Once such a blackout happens, the losses of the blackout increase with the duration of its restoration [4], and it's essential to develop an effective system restoration scheme to restore the power supply as soon as possible and minimize the adverse impacts [5-6].

The system restoration process consists of three stages: preparation, system restoration, and load recovery [6]. The objectives and constraints of the three stages are different, and a multi-stage optimization model is usually used for system restoration [7-8]. In the second stage, optimization of the restoration path is the foundation of system restoration, and can accelerate system restoration. Because the topology of a blackout system is complex and the constraints in the restoration process are strict, optimization of the restoration path is a complicated decision and control problem for system operators [9-10].

Optimization of the restoration path is a nonlinear and constrained optimization problem, which is a NP-complete problem and hard to solve. In order to reduce the difficulty of solving the problem, a mixed integer linear model was built to obtain the starting sequence of non-blackout-start (NBC) units, and then search the restoration path [11]. However, some factors such as recovery time of transmission lines are not included in the mixed integer linear model, which makes the optimal results not suitable for actual systems. Thus, optimization of the restoration path is usually modelled as a nonlinear problem. A priority index based on the complex network theory was proposed in [12] to select the restoration sequence of transmission lines considering capacities of generators, the amounts of important loads, and importance of each transmission line. A priority index based on the interpretative structural model was developed in [13] to select the restoration sequence of NBC units. The priority index can search the restoration path quickly. However, the index cannot be used for different systems. Therefore, artificial intelligence methods are

*Corresponding author.

commonly used to determine the optimal restoration path because of its modelling flexibility and excellent optimization capability. The methods used include the ant colony algorithm [14-15], particle swarm algorithm [16-17], genetic algorithm [18-21].

Because dimension of restoration path optimization is very high especially for large scale systems, and the artificial intelligent algorithms in current works are easy to be trapped in the local optima [22-23]. In order to improve the performance of the optimal solution, an effective method is to scatter individuals of the initial and offspring populations uniformly over the feasible solution space, so that the artificial intelligent algorithm can explore the whole solution space evenly [24]. The orthogonal genetic algorithm (OGA) has been proven in [25] that it can generate the initial and offspring populations scattered uniformly in the solution space.

Therefore, the contribution of this paper is proposing an OGA-based method for optimizing the restoration path of a blackout system. The OGA include the orthogonal array generation and orthogonal crossover operation which are employed to generate initial population and offspring population based on the orthogonal experimental design [26]. Because the orthogonal experimental design can search the solution space in a statistically sound manner, the initial and offspring population is a small but representative set of combinations uniformly scattered over the space of all possible combinations. As such, the optimal solution obtained by the OGA based method will be better than the traditional genetic algorithm and has been widely used in multimedia multicast routing [25], integer linear bi-level programming problems [27], packing problem [28], et al.

This paper is organized as follows: Section II describes the optimization model of power system restoration path. Section III delineates the optimization of power system restoration path based on orthogonal genetic algorithm. Section IV demonstrates the applicability and adaptability of orthogonal genetic algorithm. Finally, the conclusion is presented in section V.

2. Optimization Method of Power System Restoration Path

This section introduces the optimization model of power system restoration path and the solution method using the artificial intelligence algorithm.

2.1. Optimal Model of Power System Restoration Path

2.1.1. Objective function

The task of system restoration is to restore all black-out power plants as quickly as possible, which means that the total restoration time needs to be minimized for system restoration. The actual restoration time is affected by many factors such as transmission line operation time, unit ramping, load recovery and uncertainties. In general, the objective of optimizing power system restoration path is minimizing restoration operation costs which can be represented by the sum of energized edge weights [29].

The objective function of restoration path optimization can be described using the graph theory as follows: the post-outage system topology is abstracted as an undirected weighted graph $G = (V, E, f)$, in which V is the set of all nodes, E is the set of all edges and f is the weight set of edges; one restored node and several target nodes compose a subset S from V ; the objective is to find a connected subgraph of G that contains all the nodes of subset S and minimize the path cost. The objective function is formulated as

$$\min F = \sum_{e \in E} f(e)c(e) \quad (1)$$

where $f(e)$ denotes the weight of line e , and $c(e)$ denotes the operation status of line e . $c(e)$ is a binary variable representing whether e is in the connected subgraph or not, 1 represents in the subgraph and 0 represents not in the subgraph.

2.1.2. Constraints

In the restoration process, the restoration of generators, buses and transmission lines must meet security constraints, such as start-up power requirement constraint, critical minimum and maximum interval constraints, overvoltage constraint, power flow constraints, network security constraints, and topological constraint [12].

a) The critical minimum and maximum interval constraints:

$$\begin{cases} 0 < T_{Ai} \leq T_{CH,i} \\ T_{Ai} \geq T_{CC,i} \end{cases} \quad (2)$$

Some non-blackstart units such as thermal units with drum-type boilers have the critical maximum hot-start interval and critical minimum cold-start interval [8]. Unit i can be started when the start-up time T_{Ai} is less than the maximum hot-start interval $T_{CH,i}$ or bigger than the critical minimum cold-start interval $T_{CC,i}$.

b) Start-up power requirement constraint:

$$\sum_{i=1}^{n_G} P_{CR,i} < \sum_{j=1}^{n_B} P_{CB,j} \quad (3)$$

In the initial stage of system restoration, the spare power capacity P_{CB} of energized units n_B must meet the cranking power requirement P_{CR} of restarting units n_G [8, 11]. $P_{CR,i}$ is the cranking power requirement of unit i ; $P_{CB,j}$ is the spare power capacity of unit j .

c) Overvoltage constraint:

$$\sum_{j=1}^{n_L} Q_{Lj} < \sum_{r=1}^{n_B} Q_r^{\max} \quad (4)$$

When energizing unloaded transmission lines, massive reactive power Q_L will be produced and may result in self-excitation of generators and overvoltage at the end bus of transmission lines[30]. Thus, the reactive power Q_L generated by energizing transmission lines n_L must be less than the maximum reactive power Q^{\max} absorbed by energized generators n_B . $Q_{L,j}$ is the reactive power generated by transmission line j .

d) Power flow constraints:

$$\begin{cases} P_{Gx}^{(n)} - P_{Lx} - U_x \sum_{y \in \Omega_N \cap e_{xy} \in E} U_y (G_{xy} \cos \theta_{xy} + B_{xy} \sin \theta_{xy}) = 0 \\ Q_{Gx}^{(n)} - Q_{Lx} - U_x \sum_{y \in \Omega_N \cap e_{xy} \in E} U_y (G_{xy} \sin \theta_{xy} + B_{xy} \cos \theta_{xy}) = 0 \end{cases} \quad \forall x \in \Omega_N \quad (5)$$

where Ω_N is the set of nodes in energized power grid, e_{xy} is the line between node x and y , P_{Gx} and Q_{Gx} are the active and reactive power outputs of generators in node x , P_{Lx} and Q_{Lx} are the active and reactive power demand in node x , U_x and U_y are the voltage amplitude of nodes x and y , G_{xy} and B_{xy} are the real and imaginary part of elements in the x -th row and y -th column of bus admittance matrix, and θ_{xy} is the voltage phase difference between bus x and bus y .

e) Network security constraints:

$$P_{Gx}^{\min} \leq P_{Gx} \leq P_{Gx}^{\max}, \forall x \in \Omega_N \quad (6)$$

$$Q_{Gx}^{\min} \leq Q_{Gx} \leq Q_{Gx}^{\max}, \forall x \in \Omega_N \quad (7)$$

$$U_x^{\min} \leq U_x \leq U_x^{\max}, \forall x \in \Omega_N \quad (8)$$

$$|P_{Lb}| \leq P_{Lb}^{\max}, \forall b \in \Omega_L \quad (9)$$

where P_{Gx}^{\min} , P_{Gx}^{\max} , Q_{Gx}^{\min} , Q_{Gx}^{\max} are the minimum and maximum active power, and minimum and maximum reactive power of generators at node x , respectively. If there is no generator at node x , all the limits are set as 0. U_x^{\min} and U_x^{\max} are the minimum and maximum magnitude of the voltage of node x . Equation (9) and (10) ensure that active power flow in transmission lines must be limited within the corresponding safety range, in which Ω_L is the set of the transmission lines in the restored regions, P_{Lb} is the active power flow in transmission line b , P_{Lb}^{\max} is the power limit of transmission line b due to overheat limit of transmission line.

f) Topological constraint:

Besides the security constraints, the topological constraint is a very important constraint to ensure that the energized system is connected. This constraint is not included in the current research and usually checked by a connectivity checking algorithm [16].

2.2. Solution Method Analysis

Because the intelligent algorithm has strong ability to solve nonlinear and constrained optimization problems, the intelligent algorithm, such as the ant colony algorithm [14-15], particle swarm algorithm [16-17] and genetic algorithm [18-21], have been employed to solve the optimization model of restoration path introduced above. However, when the dimension of restoration path optimization is very high especially for large scale systems, artificial intelligent algorithms are easy to be trapped in the local optima [22-23]. An effective way to solve the problem is to increase the diversity of populations in iterations [24-25]. Therefore, an orthogonal genetic algorithm is employed to optimize the restoration path which can search the solution space in a statistically sound manner.

3. Optimization of Power System Restoration Path Based on Orthogonal Genetic Algorithm

In this section, the orthogonal experimental design is introduced first to generate the initial population, and the orthogonal crossover algorithm is employed to generate the offspring population of the GA. Then the orthogonal genetic algorithm including the generation of initial and offspring populations is applied to optimize power system restoration path.

3.1. Orthogonal Experimental Design

For an optimal problem with N factors and Q levels, there are Q^N combinations of solutions. When Q and N are very large, it's impossible to experiment all the combinations. Therefore, it's necessary to search a small but representative set of combinations for calculation. The orthogonal experimental design is an effective method [25] developed to search the small but representative set of combinations which is called the orthogonal array in the method. The orthogonal array can be expressed as $L_M(Q^N)$, in which L denotes a Latin square and M is the number of combinations in the representative set. Taking $N=3$ and $Q=2$ as an example, the number of all the combinations is $2^3=8$, and the

selected combinations for the orthogonal array is shown in Figure 1. The selected combinations are scattered uniformly over the space of all possible combinations. The orthogonal experimental design generating the orthogonal array has been proven optimal for additive and quadratic models, and the selected combinations are good representatives for all of the possible combinations [26].

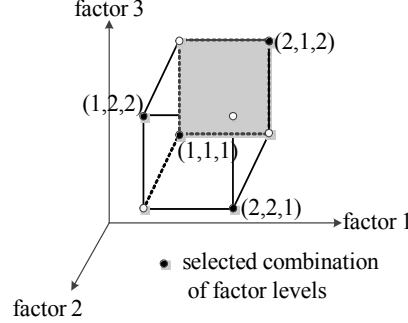


Fig. 1. Selected combinations for orthogonal array $L_4(2^3)$

3.2. Constructing Orthogonal Array and Initial Population by Orthogonal Experimental Design

The optimization problem of power system restoration path is a two-level and multi-factor problem. The factor N represents the transmission lines in the power grid and the level Q refers to the operation state of each line. The orthogonal experimental design can generate a small amount of individuals uniformly distributed in the solution space. For this reason, the orthogonal experimental design is employed to ensure uniform distribution of the initial population.

In this subsection, a simple permutation method is employed to construct orthogonal arrays [24]. $L_M(Q^N)$ is an orthogonal array with N factors and Q levels, where M is the size of combinations. $M=Q^J$, where J is the smallest integer satisfying,

$$N \leq \frac{Q^J - 1}{Q - 1} \quad (10)$$

$L_M(Q^N)$ can be denoted by $[a_{ij}]_{M \times N}$, where $[a_{ij}]$ is the level of the j -th factor in the i -th combination.

The procedure of constructing the orthogonal array is as follows:

Step 1: Determine N and Q .

Step 2: Obtain J and M by (10) and $M=Q^J$, respectively.

Step 3: Determine the sets of column ordinal B for basic columns and N_B for non-basic columns of the orthogonal array.

$$B = \{1, 2, \dots, L, (Q^{J-1} - 1) / (Q - 1) + 1\} \quad (11)$$

$$N_B = \{x | x \in \{1, 2, \dots, N\} \text{ and } x \notin B\} \quad (12)$$

Step 4: Construct the basic columns of the orthogonal array. Denote the j -th column of the array $[a_{ij}]_{M \times N}$ by a_j . For $j \in B$, a_j is denoted as the basic column, and other $j \in N_B$ is denoted as non-basic columns. The algorithm for the basic column orthogonal array is,

$$a_{i,j} = \left(\frac{i-1}{Q^{J-k}} \right) \bmod Q, \quad i=1,L \quad M, k=1,L \quad J, j \in B \quad (13)$$

Step 5: Construct non-basic columns according to the basic columns obtained from Step 3. The algorithms are as follows:

$$\begin{aligned} a_{j+(s-1)(Q-1)+t} &= (a_s \times t + a_j) \bmod Q, \\ k &= 2,L \quad J, s=1,L \quad j \\ t &= 1,L \quad Q-1, j \in B, \\ (j+(s-1)(Q-1)+t) &\in N_B \end{aligned} \quad (14)$$

Step 6: Increment $a_{i,j}$ by one for all $1 \leq i \leq M$ and $1 \leq j \leq N$. Items less than 1 are reduced to 1, and items greater than or equal to 1 are reduced to 2.

Step 7: Finally, delete redundant columns according to the size of orthogonal array required for initial population. The orthogonal experimental design can produce M combinations out of Q^N combinations. The M combinations can generate the same number of individuals, but the number of individuals in initial populations is fixed. Among the M combinations, K individuals having the best fitness value are selected as the initial population, where K is the size of initial population. Before calculating fitness value, the individual should be corrected if the topological constraint is not satisfied. The detailed correcting method can be found in reference [7].

3.3. Generate Offspring Population by Orthogonal Crossover Operation

Crossover operation is a basic operation in the GA. Strings of the parent individuals are exchanged randomly in the existing research of restoration path optimization such that new individuals of the offspring population can't be ensured to scatter uniformly in the solution space. Therefore, the orthogonal crossover operation based on the orthogonal experimental design is employed in this subsection to generate offspring population.

If M_1 individuals are to be generated as candidate offspring individuals, the optimal problem will be with N_1 factors and Q_1 levels according to the orthogonal array $L_{M_1}(Q_1^{N_1})$. For orthogonal crossover operation, Q_1 means the number of parent individuals and N_1 means the parts into which parent individuals need to be divided. Taking the orthogonal array $L_4(2^3)$ for example, there are 2 parents individuals, which need to be divided into 3 parts for crossover. And then the construction method of orthogonal array is employed to generate 4 candidate offspring individuals which are scattered more uniformly than the traditional crossover algorithm. The details are given as follows:

Step 1: According to the number of candidate offspring individuals M_1 , choose Q_1 parent individuals, $x_i = (x_{i1}, x_{i2}, \dots, x_{iN})$, $1 \leq i \leq Q_1$. The number of genes in an individual is N .

Step 2: According to divided parts N_1 of parent individual, randomly and independently generate a packet label $p(j) \in \{1, 2, \dots, N_1\}$, $1 \leq j \leq N$, for every gene in parent individuals. The gene with the packet label compose the new factor $a_{i,k}$, $1 \leq k \leq N_1$. The parent individuals can be expressed as $x_i = (a_{i1}, a_{i2}, \dots, a_{iN_1})$, $1 \leq i \leq Q_1$. The crossover operation of the GA can be transformed to the generation of orthogonal arrays with N_1 factors and Q_1 levels.

Step 3: The construction method of orthogonal array in subsection 3.2 is employed to generate M_1 candidate offspring individuals.

In general, there are more candidate offspring individuals than expected offspring individuals. The candidate offspring individuals should be corrected to satisfy the topological constraint first, and then the individuals with the best fitness value are selected as the offspring individual.

3.4. Orthogonal Genetic Algorithm for Optimization of Restoration Path

The details of the OGA for restoration path optimization are as follows:

Step 1: Coding. The state of transmission lines is considered as decision variables in the optimization model. A gene in an individual or a chromosome represents the state of a transmission line, which is expressed by “1” if the line will be energized, and “0” if the line won’t be energized. A set of genes which represent the states of all transmission lines ($e \in E$) compose a chromosome which is referred as individuals in this paper. Every possible combination of transmission line states constructs a local network of the blackout system.

Step 2: Generate candidate initial individuals by the orthogonal experimental design. The construction method of orthogonal array in subsection 3.2 is employed to generate a set of M combinations which is uniformly distributed in the solution space. One combination is a candidate individual for initial population of the GA.

Step 3: Calculate fitness function. Because a lot of individuals may not satisfy the topological constraint, the candidate individuals need to be corrected before calculating the fitness value. But the correcting time of an individual increases with the number of “1” state genes in the individual. In order to accelerate calculation speed, the individuals with more than 20% “1” state genes are chosen to be corrected. Similarly, the security constraints are not checked in iterations so as to accelerate calculation speed. Each candidate individuals is evaluated by the fitness function which is set as the objective function in (1).

Step 4: Select initial individuals. The number of candidate individuals is always larger than the size of initial population, especially for large scale systems. The candidate individuals with best fitness values are selected as the initial individuals according to the size of initial population.

Step 5: Generate parent individuals. The number of parent individuals is related to the number of expected offspring individuals with the relation $L_{M1}(Q_1^{N1})$. If the number of candidate offspring individual is M_1 , it’s necessary to choose Q_1 parent individuals randomly from the initial or offspring population.

Step 6: Generate candidate offspring individuals. The orthogonal crossover algorithm in subsection 3.3 is employed to generate candidate offspring individuals.

Step 7: Conduct mutation operation for candidate offspring individuals. Each candidate offspring individual needs to undergo mutation with a small probability in the GA. Every gene in the candidate offspring individual is flipped with a small probability.

Step 8: Select offspring individuals. Because the number of offspring individuals for each parent individuals is usually less than the number of candidate offspring individuals, it’s necessary to select the candidate offspring individuals. The selection method is the same as the one for initial individuals in step4.

Step 9: Generate offspring population. Because the size of offspring population S is several times larger than the number of offspring individuals j for each parent individuals, the generation of offspring individuals will be performed N/j times in each iteration to form the offspring population.

Step 10: Check the termination criterion. If the maximum iteration time is not achieved, go to Step 5. Otherwise, the GA will stop and the individuals with fitness values are recorded and ranked by the fitness value.

Step 11: Check security constraints and select restoration path. Because security constraints are not checked in iterations, it’s necessary to check the security constraints in (2)-(9) sequentially for the individuals. The constraints need to be checked when each transmission line of the restoration path is energized. Before a transmission line is energized, the amount of load pickup at the nodes of the restored system must be optimized for checking the constraints (5)-(9). The load optimization method can be found in [31]. In the method, the constraints (5)-(9) are included in the load optimization model. If the model can be solved, it means that the constraints (5)-(9) are satisfied. The individuals passed security check can be saved as candidate restoration path for dispatcher who will select a restoration path for power system restoration.

4. Case Study

To validate the proposed optimization method for restoration path based on the orthogonal genetic algorithm (OGA), the IEEE 9-bus test system is used to illustrate the calculation result of the OGA; the IEEE 118-bus test system and part of the Jiangsu power grid are employed to compare the OGA with the traditional genetic algorithm (TGA) with connectivity checking (TGC) [16] and connectivity correcting (TGR) [24]. The genetic operators in TGC and TGR adopt the method in [24]. Because the genetic algorithm is heuristic and random, each algorithm runs 100 times independently with the systems in this paper. All algorithms are implemented in MATLAB.

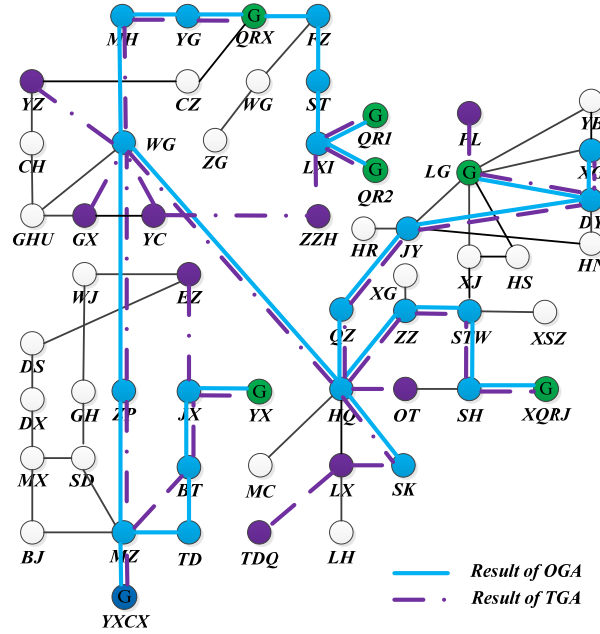


Fig. 2. Part of the Jiangsu power system and restoration path

In these cases, only one generator at a bus is specified as the blackstart generator, and other buses with generators are target nodes. The weight coefficient $f(e)$ is the charging reactive power of each transmission line [28]. The objective function is to minimize the weighted restoration paths and meanwhile satisfy the constraints (2)~(9). The topology of part of the Jiangsu power grid is shown in Fig.2. This system has 86 buses and 110 transmission lines, in which 7 nodes are generator nodes with one generator at each node. The parameters of the system for the next calculation are listed in the Appendix. The blackstart generator is located at the node of YXCX which is a pumped storage power plant.

4.1. Calculation Results of OGA

The IEEE 9-bus system with 9 buses and 9 transmission lines is employed to illustrate the calculation results of the OGA.

Table 1

Candidate Initial Individuals of IEEE 9-Bus System

Combination	Factor								
c1:	0	0	0	0	0	0	0	1	1
c2:	0	0	0	1	1	1	1	0	0
c3:	0	0	0	1	1	1	1	1	1
c4:	0	1	1	0	0	1	1	0	0
c5:	0	1	1	0	0	1	1	1	1
c6:	0	1	1	1	1	0	0	0	0
c7:	0	1	1	1	1	0	0	1	1

c8:	1	0	1	0	1	0	1	0	1
c9:	1	0	1	0	1	0	1	1	0
c10:	1	0	1	1	0	1	0	0	1
c11:	1	0	1	1	0	1	0	1	0
c12:	1	1	0	0	1	1	0	0	1
c13:	1	1	0	0	1	1	0	1	0
c14:	1	1	0	1	0	0	1	0	1
c15:	1	1	0	1	0	0	1	1	0

Table 2

The Best 4 Individuals as Initial Population

Combination	Factor								
x1:	0	0	1	1	1	1	1	1	1
x2:	1	1	1	0	1	1	1	1	1
x3:	1	1	1	1	1	0	1	1	1
x4:	1	0	1	1	1	1	1	1	1

4.1.1. Generate the initial population

Optimization of the restoration path for IEEE 9-bus system is a 2 level and 9 factor problem. Therefore, The candidate initial individuals shown Table 1 is generated by orthogonal array $L_{15}(2^9)$ using the algorithm (2)~(5).

The population size in this case is 4. Therefore, correct these candidate initial individuals first and select best 4 individuals as initial population listed in Table 2.

4.1.2. Generate offspring individuals by orthogonal crossover operation

$L_9(3^4)$ is selected to generate candidate offspring individuals by orthogonal crossover operation. The number of parent individuals is 3, which is randomly chosen from the initial population. The algorithm is repeated 2 times. The selected parent individuals are listed in Table 3 for once orthogonal crossover operation.

Table 3

The selected Parent Individual for Once Orthogonal Crossover Operation

Combination	Factor								
x1:	1	0	1	1	1	1	1	1	1
x2:	1	1	1	1	1	0	1	1	1
x3:	0	0	1	1	1	1	1	1	1
x4:	1	0	1	1	1	1	1	1	1

Table 4

Candidate Offspring Individuals of the IEEE 9-bus System

Combination	Factor								
c1:	1	0	1	1	1	1	1	1	1
c2:	1	1	1	1	1	0	1	1	1
c3:	0	0	1	1	1	1	1	1	1
c4:	1	1	1	1	1	1	1	1	1
c5:	1	0	1	1	1	1	1	1	1
c6:	0	0	1	1	1	0	1	1	1
c7:	1	0	1	1	1	0	1	1	1
c8:	1	1	0	1	1	1	1	0	1
c9:	0	1	1	1	1	1	1	1	1

Because the divided parts N_1 of parent individual is 4, generate a packet label $p = (2, 3, 4, 4, 1, 4, 4, 2, 4)$ for parent individuals and divide each parent into 4 parts. And then the orthogonal crossover operation in subsection 2.3 is executed to generate candidate offspring individuals which are listed in Table 4.

After the orthogonal crossover operation, mutation operation is executed. And then the candidate offspring individuals generated by 2 times are corrected and the best 4 individuals are selected as offspring individuals.

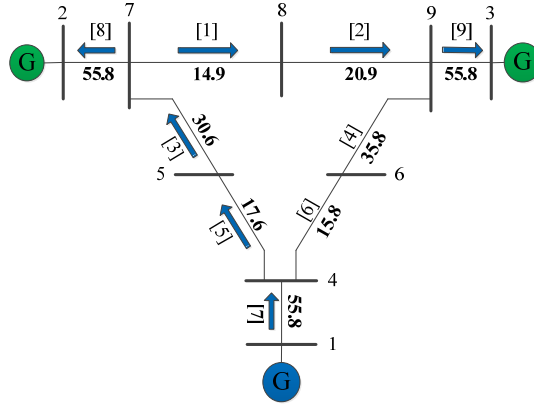


Fig. 3. The optimal restoration path searched by OGA for IEEE 9-bus system

4.1.3. Obtain the optimal result

While the maximum iteration time is reached, the individuals with best fitness values will be chosen to check the security constraints. The first individual satisfying security constraints will be chosen to be the optimal result. In this case, the optimal result of OGA is $x_1=(1, 1, 1, 0, 1, 0, 1, 1, 1)$.

The optimal restoration path mapped by x_1 is shown in Fig. 3. The generator in the bus 1 is the blackstart generator and the bus “2” and “3” are specified as target nodes. The number in square brackets “[]” represents the number of transmission lines, and the numbers in bold indicate the weight of lines. The blue arrow represents optimal restoration path with the path weight 251.4.

4.2. Comparison of OGA, TGC, and TGR

4.2.1 Comparison of optimization results

The OGA, TGC, and TGR algorithms are tested 100 times independently with the IEEE 118-bus test system, IEEE 300-bus test system and part of the Jiangsu power grid. The recorded data include the minimum value of objective function, the maximum value of objective function and the average value of objective function in the 100 tests. Statistics are listed in Table 5.

From Table 5, it can be seen that the OGA’s minimum value of the objective function is less than TGC’s and TGR’s in the three systems. It means that the OGA is better than the other two methods for finding the optimal value. In addition, the OGA’s maximum and average value of the objective function in 100 tests is also less than the two other methods. These results indicate that the OGA’s solution is steadier. In another word, the deviation of the tests is smaller. Therefore, the OGA has a higher probability to obtain a better result.

For the Jiangsu 86-bus system, the restoration paths obtained by the OGA and TGR are compared in Fig.2, in which the solid line and dot-dash line represent the results of the OGA and TGR, respectively. The value of the objective function for the restoration path obtained by the OGA is 1508.6, which is less than 1521.5 obtained by the TGR. This also confirms that the proposed method can search a better restoration path.

Table 5

The Comparison of Optimization Results between OGA, TGC and TGR

System	Algorithm	The Objective Function Value		
		Minimum	Maximum	Average
IEEE 118-bus	TGC	1033.6	1396.9	1187.9
	TGR	981.0	1093.1	1011.0
	OGA	963.5	993.1	974.6
IEEE 300-bus	TGC	13616.4	16661.9	15300.8
	TGR	10322.6	12323.1	11584.6

Jiangsu 86-bus	OGA	10152.1	10573.1	10310.3
	TGC	1557.4	2296.1	1996.7
	TGR	1521.5	1640.7	1533.0
	OGA	1508.6	1530.2	1521.3

Table 6

Comparison of Solution Quality for Jiangsu 86-bus System

Method	The number of tests whose cost are within x% of optimal value				
	x=20	x=10	x=5	x=2	x=0
TGC	14	3	1	0	0
TGR	100	100	99	92	0
OGA	100	100	100	100	1

Table 7

Comparison of Solution Quality for IEEE 118-bus System

Method	The number of tests whose cost are within x% of optimal value				
	x=20	x=10	x=5	x=2	x=0
TGC	41	5	0	0	0
TGR	100	97	64	2	0
OGA	100	100	100	88	1

Table 8

Comparison of Solution Quality for the IEEE 300-bus System

Method	The number of tests whose costs are within x% of optimal value				
	x=20	x=10	x=5	x=2	x=0
TGC	0	0	0	0	0
TGR	98	12	1	1	0
OGA	100	100	100	93	1

4.2.2. Comparison of solution quality

In order to measure the solution quality, the percentage of tests, whose objective function values are within x% of the optimal value, are recorded. The optimal value is the minimum objective function value of three algorithms in the 300 tests. The result statistics are listed in Tables 6-8.

In Tables 6- 8, it is seen that the proposed OGA can find the minimum objective function value in all the three test systems. However, the TGC can only search 3 and 5 solutions within 10% of optimum respectively, and can't search the solution within 20% of the optimum for the IEEE 300-bus system. Though the TGR has a better performance than the TGC, the number of solution within 2% of optimum for TGR is only 2 times and 1 time for the IEEE 118-bus system and 300-bus system, respectively. In the same cases, the OGA algorithm can find 88 and 93 solutions within 2% of the optimum. It indicates that the OGA has better solution quality than the TGC and TGR.

4.2.3. Comparison of convergence property

Table 9

The Comparison of Convergence Property for Jiangsu 86-bus System

Method	Mean number of generations required to search a solution whose cost is within x% of optimal value				
	x=20	x=10	x=5	x=2	x=0
TGC	40.7	53.3	82.0	Na	Na
TGR	12.8	22.8	39.0	50.6	Na
OGA	1	1	1	13.1	82.0

Table 10

The Comparison of Convergence Property for IEEE 118-bus System

Method	Mean number of generations to search a solution whose cost is within x% of optimal value				
--------	--	--	--	--	--

	x=20	x=10	x=5	x=2	x=0
TGC	3.5	4.0	Na	Na	Na
TGR	3.2	22.9	66.0	86.0	Na
OGA	1	7.3	13.6	24.2	32.0

Table 11

The Comparison of Convergence Property for the IEEE 300-bus System

Method	Mean number of generations to search a solution whose cost is within x% of optimal value				
	x=20	x=10	x=5	x=2	x=0
TGC	Na	Na	Na	Na	Na
TGR	43.4	83.5	94.0	99.0	NaN
OGA	4.1	7.1	9.8	16.8	27.0

In order to compare the convergence property of the three algorithms, the mean number of generations required to search a solution whose cost within x% of the optimal has been listed in Tables 9-11. The best converge curve of three algorithms in the tests is shown in Figures 4-6.

The result statistics in Tables 9-11 show that the mean number of generations required for the OGA is less than TGC and TGR. For larger systems, the mean number of generations required for OGA is smaller than other two algorithms. The number of generations for larger system to obtain the optimal result by OGA is less than the number of generations for smaller system. Together with the results in Tables 6-8, the OGA proposed in this paper has a better solution quality and a faster convergence speed than the TGC and TGR.

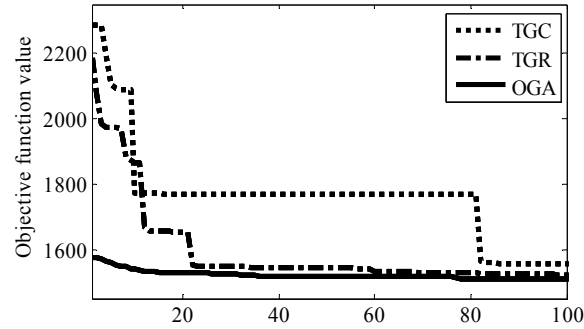


Fig. 4. Convergence curve of the Jiangsu 86-bus System

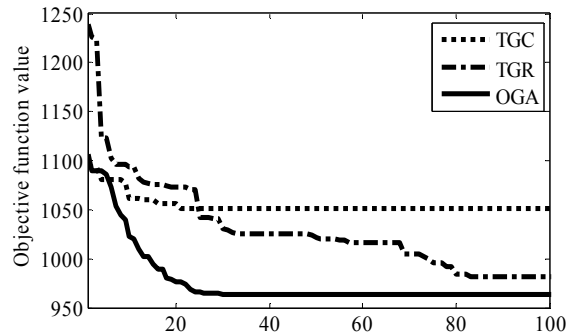


Fig. 5. Convergence curve of the IEEE 118-bus system

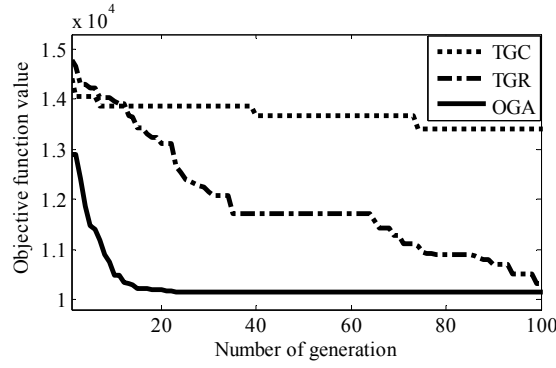


Fig. 6. Convergence curve of the IEEE 300-bus system

From Figures 46, the three algorithms can be compared from 3 aspects: initial value, convergence rate and convergence precision. The initial value of the OGA is generated by the orthogonal experimental design. The initial value of the OGA is much better than other two algorithms in Figure 4 and 6, and not worse than the other two algorithms in figure 5. It confirms the effectiveness of the orthogonal experimental design. The convergence rate of the OGA is much faster than the other two algorithms because the orthogonal crossover operation is employed to generate offspring population. The convergence precision of the OGA is better because the offspring individuals are scattered in the solution space more evenly. It is also shown in Table 5.

4.3. The case for abnormal incidents

One of the major reasons for the power system blackout is natural disasters, e.g., the Hainan power system blackout on September 26, 2005 was caused by the Damrey typhoon. Some transmission towers were destroyed by the typhoon, which cannot be quickly repaired. The transmission lines with destroyed transmission tower should be neglected in the optimization of the restoration scheme. Take part of the Jiangsu power system as an example, if the transmission line WN-MH and HQ-CZ are destroyed by the natural disaster, the new restoration path generated by the OGA is shown in Figure R2 by the red dot line.

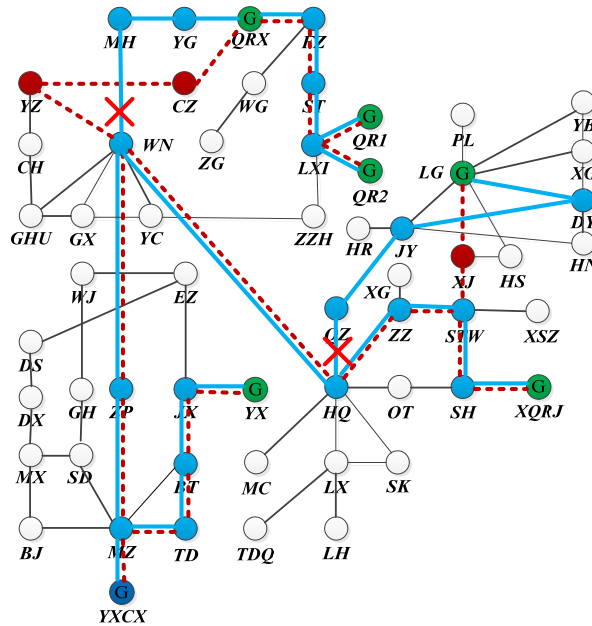


Fig. 7. The new restoration path for part of the Jiangsu power system with destroyed transmission lines

Compare the new restoration path with the original one, the transmission lines with destroyed transmission towers are removed from the restoration path. The value of the objective function for the new restoration path obtained by the OGA is 1509.6, which is larger than 1508.6 which is the value of the original restoration path. This further confirms that the proposed method can find a better restoration path.

5. Conclusion

Fast optimization of the power system restoration path has important and practical significance for power system restoration. Because the dimension of restoration path optimization is very high, especially for large scale systems, current artificial intelligent algorithms are easy to be trapped in the local optima. An orthogonal genetic algorithm is developed to generate the initial and offspring population in this paper, which scatters the individuals of initial and offspring populations uniformly over the feasible solution space so that the algorithm can explore the whole solution space evenly. Simulation results demonstrate that the proposed method can find better restoration paths than traditional genetic algorithms. Similarly, solution quality and convergence speed of the orthogonal genetic algorithm are better than traditional genetic algorithms. The method in this paper can be used for the practical application in the optimization of restoration path.

References

- [1] Sudhakar T D, Srinivas K N. Restoration of power network—a bibliographic survey. *International Transactions on Electrical Energy Systems*, 2011, 21(1): 635-655. Doi:10.1002/etep.467.
- [2] Andersson G, Donalek P, Farmer R, et al. Causes of the 2003 major grid blackouts in North America and Europe, and recommended means to improve system dynamic performance. *IEEE Transactions on Power Systems*, 2005, 20(4): 1922-1928.
- [3] Romero J J. Blackouts illuminate India's power problems. *IEEE spectrum*, 2012, 49(10): 11-12.
- [4] Adibi M M, Fink L H. Overcoming restoration challenges associated with major power system disturbances-Restoration from cascading failures. *IEEE Power and Energy Magazine*, 2006, 4(5): 68-77.
- [5] Abbaszadeh A, Abedi M, Doustmohammadi A. General Stochastic Petri Net approach for the estimation of power system restoration duration. *International Transactions on Electrical Energy Systems*, 2018.
- [6] Wang D, Gu X, Zhou G, et al. Decision - making optimization of power system extended black - start coordinating unit restoration with load restoration. *International Transactions on Electrical Energy Systems*, 2017, 27:e2367. Doi:10.1002/etep.2367
- [7] Y. H. Hou, C. C. Liu, K. Sun, et al. Computation of Milestones for Decision Support During System Restoration. *IEEE Transactions on Power Systems*, 2011, 26(3): 1399-1409.
- [8] Gu X, Zhong H. Optimisation of network reconfiguration based on a two-layer unit-restarting framework for power system restoration. *IET generation, transmission & distribution*, 2012, 6(7): 693-700.
- [9] Shen C, Kaufmann P, Hachmann C, et al. Three-stage power system restoration methodology considering renewable energies. *International Journal of Electrical Power & Energy Systems*, 2018, 94: 287-299.
- [10] Pan Z, Zhang Y. A flexible black - start network partitioning strategy considering subsystem recovery time balance. *International Transactions on Electrical Energy Systems*, 2015, 25(8): 1644-1656. Doi: 10.1002/etep.1932.
- [11] Golshani A, Sun W, Zhou Q, et al. Incorporating Wind Energy in Power System Restoration Planning. *IEEE Transactions on Smart Grid*, 2017.
- [12] Lin Z, Wen F, Xue Y. A restorative self-healing algorithm for transmission systems based on complex network theory. *IEEE Transactions on Smart Grid*, 2016, 7(4): 2154-2162.
- [13] Zhang C, Sun L, Wen F, et al. An interpretative structural modeling based network reconfiguration strategy for power systems. *International Journal of Electrical Power & Energy Systems*, 2015, 65: 83-93.
- [14] Ketabi A, Feuillet R. Ant colony search algorithm for optimal generators startup during power system restoration[J]. *Mathematical Problems in Engineering*, 2010: 1-11.

- [15] Chou Y T, Liu C W, Wang Y J, et al. Development of a black start decision supporting system for isolated power systems. *IEEE Transactions on Power Systems*, 2013, 28(3): 2202-2210.
- [16] Liu Y, Gu X. Skeleton-network reconfiguration based on topological characteristics of scale-free networks and discrete particle swarm optimization[J]. *IEEE Transactions on Power Systems*, 2007, 22(3): 1267-1274.
- [17] Sun L, Wang X, Liu W, et al. Optimisation model for power system restoration with support from electric vehicles employing battery swapping. *IET Generation, Transmission & Distribution*, 2016, 10(3): 771-779.
- [18] Lakshminarayana C, Mohan M R. A genetic algorithm multi - objective approach for efficient operational planning technique of distribution systems. *International Transactions on Electrical Energy Systems*, 2009, 19(2): 186-208. Doi:10.1002/etep.206.
- [19] Vitorino R M, Jorge H M, Neves L P. Multi - objective optimization using NSGA - II for power distribution system reconfiguration[J]. *International Transactions on Electrical Energy Systems*, 2015, 25(1): 38-53. Doi: 10.1002/etep.1819.
- [20] El-Zonkoly A M. Renewable energy sources for complete optimal power system black-start restoration. *IET Generation, Transmission & Distribution*, 2014, 9(6): 531-539.
- [21] Salehi J, Haghifam M R. Determining the optimal reserve capacity margin of Sub - Transmission (ST) substations using Genetic Algorithm. *International Transactions on Electrical Energy Systems*, 2014, 24(4): 492-503.
- [22] Styblinski M A, Tang T S. Experiments in nonconvex optimization: stochastic approximation with function smoothing and simulated annealing. *Neural Networks*, 1990, 3(4): 467-483.
- [23] Siarry P, Berthiau G, Durdin F, et al. Enhanced simulated annealing for globally minimizing functions of many-continuous variables. *ACM Transactions on Mathematical Software (TOMS)*, 1997, 23(2): 209-228.
- [24] Zhang Q, Leung Y W. An orthogonal genetic algorithm for multimedia multicast routing. *IEEE Transactions on Evolutionary Computation*, 1999, 3(1): 53-62.
- [25] Leung Y W, Wang Y. An orthogonal genetic algorithm with quantization for global numerical optimization. *IEEE Transactions on Evolutionary computation*, 2001, 5(1): 41-53.
- [26] Wu Q. On the optimality of orthogonal experimental design. *Acta Math. Appl. Sinica*, 1978, 1(4): 283-299.
- [27] Li H, Zhang L, Jiao Y. Solution for integer linear bilevel programming problems using orthogonal genetic algorithm. *Journal of Systems Engineering and Electronics*, 2014, 25(3): 443-451.
- [28] Gonçalves J F, Resende M G C. A parallel multi-population genetic algorithm for a constrained two-dimensional orthogonal packing problem. *Journal of Combinatorial Optimization*, 2011, 22(2): 180-201.
- [29] Shi L B, Ding H L, Xu Z. Determination of weight coefficient for power system restoration. *IEEE Transactions on Power Systems*, 2012, 27(2): 1140-1141.
- [30] Wang C, Vittal V, Kolluri V S, et al. PTDF-based automatic restoration path selection[J]. *IEEE Transactions on Power Systems*, 2010, 25(3): 1686-1695.
- [31] Gholami A, Aminifar F. A hierarchical response-based approach to the load restoration problem. *IEEE Transactions on Smart Grid*, 2017, 8(4): 1700-1709.

Appendix A

Table A1

Parameters of the generators in the Jiangsu 86-bus System

Unit ID	Maximum power (MW)	Cranking power (MW)	Ramp rate (MW/min)	Maximum reactive power (MVAR)
YXCX	1000	5.000	/	150.0
YX	270	10.03	1.7298	92.71
QR1	390	14.54	3.5028	246.5
QR2	390	14.74	3.5809	246.5
QRX	420	20.42	4.9296	92.98
XQRJ	796	7.960	7.5174	247.0
LG	740	30.10	4.9296	216.9

Table A2

Parameters of the loads at the nodes of the Jiangsu 86-bus System

Node ID	Maximum active load (MW)	Maximum reactive load (MVAR)	Node ID	Maximum active load (MW)	Maximum reactive load (MVAR)
WG	105.0	21.00	LXI	180.0	36.00
MZ	27.84	0.040	SH	150.0	30.00
EZ	160.0	32.00	JX	160.0	32.00
QZ	165.0	33.00	SK	195.0	39.00
ZZ	150.0	30.00	BT	135.0	27.00
LX	180.0	36.00	SD	120.0	24.00
STW	150.0	30.00	GX	148.0	29.60
SG	180.0	36.00	YZ	118.0	23.60
JY	140.0	28.00	YB	85.00	17.00
TD	85.00	17.00	XJ	150.0	30.00
MX	145.0	29.00	XSZ	60.00	12.00
FZ	102.0	20.40	RG	100.0	20.00
YG	163.0	32.60	XG	30.00	6.000
GHU	208.0	40.00	ZZH	102.0	20.40
TDQ	160.0	32.00	GH	120.0	24.00
YC	177.0	35.40	WG	330.0	66.00
DX	150.0	30.00	ST	50.00	10.00
HN	190.0	38.00	HS	40.00	8.000
DY	175.0	35.00	OT	75.00	20.00
BJ	145.0	29.00	DS	30.00	6.000
WJ	130.0	26.00	CH	100.0	20.00
MH	114.0	22.80	LH	80.00	16.00
LG	14.70	5.000	YX	7.840	3.000

Table A3

The weight coefficient of the transmission lines in the Jiangsu 86-bus System

Node1	Node2	Weight	Node1	Node2	Weight	Node1	Node2	Weight	Node1	Node2	Weight
WN	HQ	24.332	LG	PL	1.016	LXI	QR1	2.98	MZ	BT	4.2
YXCX	MZ	6.788	LG	XJ	7.27	LXI	QR2	2.98	MZ	SD	2.756
WN	ZP	8.372	LG	YB	1.652	QRX	YG	0.31	MZ	TD	2.64
MZ	ZP	68.926	DY	LG	0.31	STW	XSZ	0.676	JY	HR	0.644
WN	MZ	85.098	LG	JY	6.274	STW	SH	0.928	JY	QZ	4.736
BJ	MX	4.828	YX	JX	0.31	STW	ZZ	1.55	XQRJ	SH	1.008
EZ	WJ	2.17	LX	SK	1.202	SD	GH	1.338	DX	DS	1.612
FZ	WG	1.094	LX	TDQ	1.064	TD	BT	1.65	HS	XJ	5.442
GX	GHU	1.726	LXI	ZZH	2.148	ZG	WG	0.31	HQ	OT	3.224
XG	DY	0.31	MH	YG	1.22	XJ	STW	1.272	LG	HS	3.024
GH	WJ	1.114	MX	DX	3.136	YB	XG	1.02	LXI	ST	2.52
HQ	LX	3.226	MX	SD	2.194	CZ	YZ	1.246	OT	SH	3.224
HQ	MC	1.194	GHU	WN	2.012	HN	JY	0.31	ST	FZ	2.52
HQ	QZ	2.85	GX	WN	1.428	DY	JY	0.31	CH	GHU	2.016
HQ	SK	1.282	MH	WN	0.756	DY	HN	6.042	CH	YZ	2.016
HQ	ZZ	1.592	YZ	WN	0.888	YC	GX	1.908	LX	LH	2.978
JX	BT	0.31	YC	WN	2.602	ZZ	XG	0.688	DS	EZ	3.024
JX	EZ	2.096	CZ	QRX	1.25	YC	ZZH	1.528			
XG	LG	1.798	QRX	FZ	0.838	MZ	BJ	4.358			